

# Synchronized oscillation in a modular neural network composed of columns

LI Su<sup>1</sup>, QI Xianglin<sup>1</sup>, HU Hong<sup>2</sup> & WANG Yunjiu<sup>1</sup>

1. Laboratory for Visual Information Processing, Institute of Biophysics, Chinese Academy of Sciences, Beijing 100101, China;

2. Institute of Computing Technology, Chinese Academy of Sciences, Beijing 100080, China

Correspondence should be addressed to Wang Yunjiu (email: yjWang@sun5.ibp.ac.cn)

Received November 13, 2003; revised May 11, 2004

**Abstract** The columnar organization is a ubiquitous feature in the cerebral cortex. In this study, a neural network model simulating the cortical columns has been constructed. When fed with random pulse input with constant rate, a column generates synchronized oscillations, with a frequency varying from 3 to 43 Hz depending on parameter values. The behavior of the model under periodic stimulation was studied and the input-output relationship was non-linear. When identical columns were sparsely interconnected, the column oscillator could be locked in synchrony. In a network composed of heterogeneous columns, the columns were organized by intrinsic properties and formed partially synchronized assemblies.

**Keywords:** cortical column, synchronized oscillation, Rose-Hindmarsh model.

**DOI:** 10.1360/03yc0240

Since it was first reported in 1957<sup>[1]</sup>, the columnar organization has been found in somatic sensory cortex, visual cortex, auditory cortex, motor cortex and association cortex of various different species including mice, rat, cats, rabbits, monkeys and humans<sup>[2]</sup>. These experimental findings strongly supported that the cortical columns are basic anatomical and physiological units of the cortex and suggested that columns might be of fundamental importance for the function of the brain<sup>[2,3]</sup>.

Mathematical models were constructed and simulated to investigate the biological function of the column in the information processing in the brain. Wilson-Cowan model<sup>[4]</sup> is most frequently used to simulate the electrophysiological activities of the cortical columns in the previous studies. For example, Schuster et al.<sup>[5]</sup> proposed a columnar model to simulate the synchronized oscillation discovered in visual

cortex. Jansen<sup>[6,7]</sup> presented a mathematical model of coupled cortical columns which produced EEG-like waveform and evoked potentials. Fukai<sup>[8]</sup> designed a network model in columnar structure to simulate visual pattern retrieval. Some of the column models are phase models which assume a column as an oscillator and simulate mere the phase of oscillating activities<sup>[9,10]</sup>.

There has been few modeling of columns based on spiking single neurons. By replacing the single cell as the functional unit by multiple cells in cortical columns, an attractor network model was constructed and simulated to perform associative memory<sup>[11]</sup>. Hansel and Sompolinsky<sup>[12]</sup> constructed a hypercolumn model according to the physiological organization in the orientation columns in visual cortex. The synchronous and chaotic activities in the hypercolumn were studied and the model was used to explore the cortical mechanisms for orientation selectivity.

First, to assess whether a single column model can subserve an adequate basis for the population interaction in the neocortex, it is necessary to identify its specific requirements on the network properties and its reaction to different input pattern. In this paper, we present a simplified column model with physiological significance and study its dynamic properties in terms of computer simulations. Second, a multi-column network is constructed by sparsely inter-connected column models. Interaction between equivalent and non-equivalent columns is studied and new characteristics are found in the activities of this modular network..

## 1 Model

### 1.1 Neuron model

We intended to construct a column model based on spiking neurons, so we chose the Rose-Hindmarsh (R-H) model<sup>[13]</sup> to describe the dynamics of the neurons in the model:

$$\left. \begin{aligned} \dot{x} &= y + ax^3 - bx^2 - z + I_{syn} + I_{stim}, \\ \dot{y} &= c - dx^2 - y, \\ \dot{z} &= r[s(x - x_0) - z], \end{aligned} \right\} \quad (1)$$

where  $x$  stands for the membrane potential,  $y$  is the fast recovery currents,  $z$  describes slow adaptive currents,  $I_{syn}$  means the synaptic currents from other neurons and  $I_{stim}$  means the afferent input current,  $a, b, c, d, r, s, x_0$  are constants. In this paper,  $a = 1, b = 3, c = 1, d = 5, s = 2$  and  $x_0 = -1.6$ . For the Rose-Hindmarsh neuron, the time scale is defined as 5 units of eq. (1) equaling 1 ms<sup>[13]</sup>.

According to the experimental results<sup>[14,15]</sup>, there are mainly two physiological types of cortical neurons: the excitatory regular-spiking (RS) neurons and the inhibitory fast-spiking (FS) neurons. RS neurons, which are all morphologically identified as spiny and pyramidal cells, exhibit evident and rapid firing-frequency adaption responding to a continuous depolarizing current injection; FS neurons are all non-spiny and non-pyramidal cells and they respond to long depolarizing current stimulus with higher rate of firing and less prominent spike-frequency adaption than the

former. We assign  $r_{RS} = 0.015$  and  $r_{FS} = 0.001$  in the neuron models to respectively represent their different spiking properties. The plots of instantaneous firing frequency versus time for both neurons are shown in fig. 1(a).

### 1.2 Synapse model

In this model, neurons are connected by a current-based synapse model. Each action potential in the pre-synaptic cell intrigues the synaptic current  $I_{syn}$  injection in the post-synaptic cell after a defined delay. The equation for the postsynaptic current  $I_{syn}$  is as follows:

$$I_{syn} = g_{syn} V_{syn} (e^{-t/\tau_1} - e^{-t/\tau_2}), \quad (2)$$

where  $g_{syn}$  is the conductance,  $\tau_1$  and  $\tau_2$  are time constants,  $V_{syn}$  means the synaptic voltage. In this paper  $V_{syn}$  is used to represent the coupling strength of the connections.  $V_{syn}$  of excitatory connections between RS cells is referred to as  $V_{RR}$ , and by the same token,  $V_{RF}$  and  $V_{FR}$  respectively refer to  $V_{syn}$  in the excitatory synapse from RS to FS and the inhibitory projection from FS to RS.  $g_{RR} = 4, \tau_{1(RR)} = 3, \tau_{2(RR)} = 2, g_{RF} = 8, \tau_{1(RF)} = 1, \tau_{2(RF)} = 0.7, g_{FR} = 4, \tau_{1(FR)} = 3, \tau_{2(FR)} = 2$ .  $V_{FR}$  is set to  $-1$  throughout this paper.  $V_{RR}$  and  $V_{RF}$  vary between 0.1 and 1 during the simulation. The synaptic currents and the post-synaptic membrane potentials are plotted in fig. 1(b).

### 1.3 Model architecture

The main characteristic structure of the model is that the network is composed of column modules. Instead of connecting the individual neurons directly, we first group the neurons into columns and then organize the columns into a larger neural network. The column is regarded as a relatively invariant structural unit in the network.

The architecture of the single column model is based on the physiological data but much simplified. The anatomical sampling of the neurons in the cortex shows that 80% of the neurons are excitatory and the rest 20% are inhibitory<sup>[16]</sup>. In the model, a column is composed of 15 neurons, 12 RS neurons and 3 FS neurons.

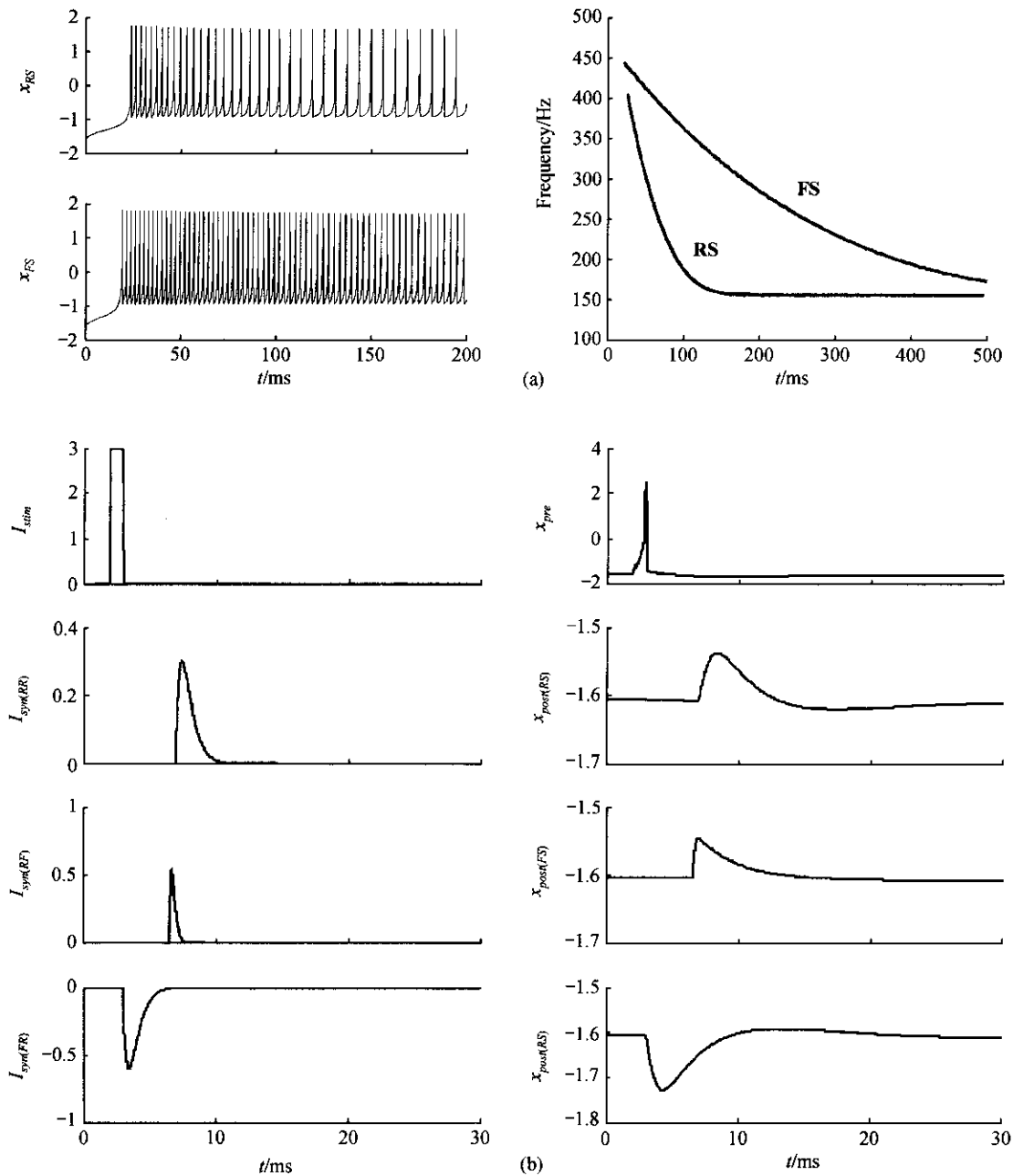


Fig. 1. The model of two kinds of single neurons and three kinds of synapses. (a) Different spiking properties of the regular-spiking (RS) neuron and fast-spiking (FS) neuron models. Left: Firing patterns of the two types of neuron models responding to continuous current injection. The stimulating current  $I_{stim}$  for two are equally 0.23 and both start at 0 ms. Right: Instantaneous firing frequency versus time of the model neurons. (b) (from top to bottom) A brief current ( $I_{stim} = 3$ ) applied to a presynaptic RS cell generates a single action potential, which elicits excitatory postsynaptic currents ( $I_{syn}$ ) and membrane potential ( $x$ ) changes in two postsynaptic cells, an RS cell and an FS cell, via RR and RF projection respectively. The inhibitory  $I_{syn}$  and  $x$  of an RS cell shown in the bottom row is postsynaptic to another activated FS cell (not shown).

In a cortical column, almost all the intrinsic excitatory synapses are imposed via the exuberant recurrent collateral branches of pyramidal cell stem axons. These branches avoid its own origin pyramidal cell and project on the dendrites of other pyramidal cells within the restricted zone of the column. By such connections, the pyramidal cells in a column are coupled into an excitatory system<sup>[3]</sup>. In the model, each RS cell is connected to 6 other randomly chosen RS cells. The latency of the projections from RS neurons to RS neurons (referred to as RR) is 1.2 units with a standard deviation of 2.5%.

The axon collaterals from pyramidal cells also terminate upon inhibitory interneurons, providing one mechanism for pericolumnar inhibition. In our model, each FS cell receives synapses from 5 RS cells, thus each RS cell contacts 1.25 cells on average. The ratio of RS cell contacting RS cells and FS cells is compatible with the statistics in the anatomical study<sup>[17]</sup>. The delay of the RF synaptic transmission is 0.8 unit with a standard deviation of 2.5%. The inhibitory interneurons each make inhibitory FR synapses onto 8 pyramidal cells with a delay of  $0.5 \pm 2.5\%$  units.

As far as the inter-columnar connections are concerned, we assume that the inhibitory cells only make local contacts while axons of RS cells can ramify their collaterals to other columns. The inter-columnar connections in our model only exist between RS neurons (termed as iRR. The prefix i means inter-column, similarly hereinafter), 2 pre-synaptic RS neurons in one column projecting to 6 post-synaptic RS neurons in another column, which is much sparser than the intra-columnar connections. Every two columns among the network are mutually connected. Parameters of the iRR synapse are  $g_{iRR} = 4$ ,  $t_{1(iRR)} = 3$ ,  $t_{2(iRR)} = 2$ , and the latency is  $1.2 \pm 2.5\%$  units.

#### 1.4 Input to the model

Randomly generated pulses were presented to the column model to simulate the spontaneous firing in the cortex and the inputs from thalamus and other cortical columns. The pulses were presented to the 12 RS cells only, and independent in each cell. Each pulse

drives a depolarizing current  $I_{stim}$  on the cell stimulated which is described by the following equation:

$$I_{stim} = g_{stim} V_{stim} (e^{-t/t_1} - e^{-t/t_2}), \quad (3)$$

where  $g_{stim} = 4$ ,  $V_{stim} = 0.08$ ,  $t_{1(stim)} = 3$ ,  $t_{2(stim)} = 2$ . The stimulating current is much weaker than the synaptic one.

The stimulus intensity is defined as the probability  $P_{stim}$  of each RS cell receiving a pulse input during every time step ( $P_{stim}$  is so small that a neuron is assumed to receive only one pulse at most in one step).  $P_{stim}$  is a constant for continuous invariant stimuli. When periodic stimuli are presented,  $P_{stim}$  is defined as a function of  $t$  as follows:

$$P_{stim}(t) = E_{stim} + A_{stim} \cdot \sin(\omega t \cdot 2\pi/T). \quad (4)$$

$E_{stim}$  and  $A_{stim}$  are respectively the mean and the amplitude of sinusoidal oscillation of  $P_{stim}$ .  $T$  equals 5000 units which in the model is equivalent to 1, so  $\omega$  is the frequency of the pulse probability wave after the time scale of the model has been converted to units of seconds.

#### 1.5 Measurements and numerical methods

The local field potential of a column is defined as the running average of all membrane potentials of 12 RS cells. The power spectrum of output activity is calculated by the fast Fourier transform of the autocorrelation function of field potential.

To quantify the synchronization of neuronal firing within a column, we introduce a synchrony measure based on the zero-lag cross-correlations of neuronal pairs in the column network<sup>[18]</sup>. A period of time  $T$  is divided into small time bins of  $I$ . The potentials within each bin are averaged and a new potential train  $X_i(l)$ ,  $l = 1, 2, 3, \dots, n$  ( $n = T/I$ ) is obtained. The zero-lag cross-correlation between two RS neurons  $i$  and  $j$  ( $1 \leq i, j \leq 12$ ) is defined as

$$k_{ij} = \frac{\sum_l (x_i(l) - \bar{x}_i)(x_j(l) - \bar{x}_j)}{\sqrt{\sum_l (x_i(l) - \bar{x}_i)^2 \sum_l (x_j(l) - \bar{x}_j)^2}}. \quad (5)$$

The population synchrony measure  $k$  is defined by the average of  $k_{ij}$  over the number of RS neural pairs in the network. In this paper, the time bin  $I$  is set to 1 unit, which equals 0.2 ms.

The column model was integrated with a time step of 0.01 ms. All the measurements were calculated after 125 ms transients. For the randomness in the network connectivity, each set of the simulations was run with three to four random realizations of the network connections.

## 2 Simulation results in a single column model

In this section, we will first demonstrate that a column is capable of acting as an oscillator. The simulation was started by feeding the model column with invariant input. The results show that bursts of discharges of pyramidal cells inside a column tend to be synchronized and the field potential of the network oscillates in specific rhythms. Fig. 2 illustrates several

kinds of activities of the column. A well-defined alpha rhythm is produced in fig. 2(a). The field potential in the middle panel exhibits typical waxing and waning amplitudes in a period of about 1.5 s. The power spectrum of the field potential indicates the frequency of the oscillation locates in alpha band (8—13 Hz). In fig. 2(b), the output of the column oscillates in beta rhythm (14—30 Hz). The activity in fig. 2(c) has the frequency of 2—11 Hz, partly in alpha frequency band, but the waveform is obviously distinguished from the one in fig. 2(a) by large amplitude and prolonged bursting phases. A 40 Hz oscillation can be seen in fig. 2(d). In fig. 2(e), the neurons in the column fire uninterruptedly. The power spectrum is broad and has no prominent peak. This noisy state will be referred to as hyperactive noise. All the aforementioned output patterns were produced by the model under different parameter conditions. In the following sections we will discuss how the parameters affect the activity of the

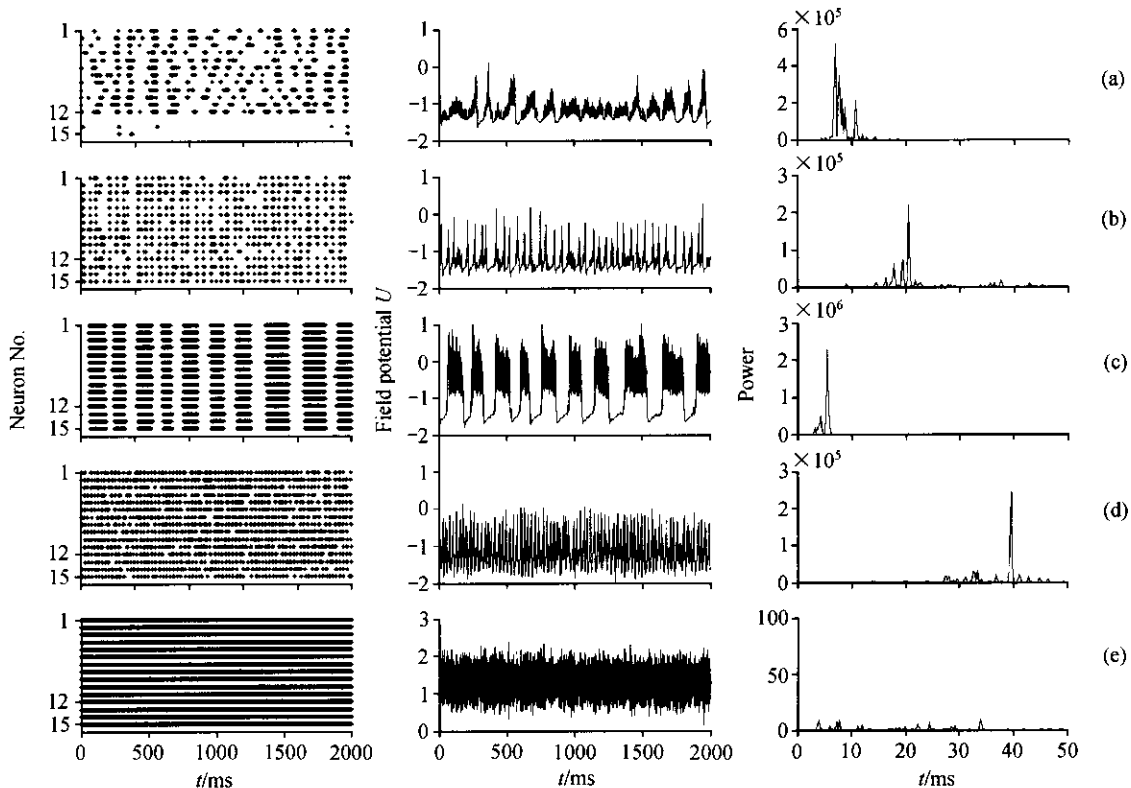


Fig. 2. Several activity patterns of the column model. Left panels: spatiotemporal firing patterns. The ordinate represents the 15 neurons, of which top 12 cells are RS cells and the rest 3 in the bottom are FS cells. Each dot indicates the occurrence of an action potential. Middle panels: Potential fields of the column model. Right panels: Power spectra of the field potentials indicating the frequency of the rhythmic output. (a)  $V_{RR} = 0.1$ ,  $V_{RF} = 0.4$ ; (b)  $V_{RR} = 0.4$ ,  $V_{RF} = 1$ ; (c)  $V_{RR} = 0.6$ ,  $V_{RF} = 0.3$ ; (d)  $V_{RR} = 0.1$ ,  $V_{RF} = 0.6$ ; (e)  $V_{RR} = 1$ ,  $V_{RF} = 0.1$ .  $P_{stim} = 0.025$  except that  $P_{stim} = 0.04$  in (d).

model.

### 2.1 Synchronization and synaptical strengths

To investigate further the dependence of the synchronized oscillation on the synaptic strength in the excitatory and inhibitory recurrent pathway, the model was simulated while  $V_{RR}$  and  $V_{RF}$  changed gradually.  $P_{stim}$  was set unchanged at 0.025. In fig. 3(a), the frequency is plotted in the two-dimensional parameter space of  $V_{RR}$  and  $V_{RF}$ . A white region can be observed at the corner of high  $V_{RR}$  and low  $V_{RF}$  in the figure, which represents the hyperactive noise as shown in fig. 2(e). While increasing  $V_{RR}$ , the oscillating frequency of the column increases at first, then decreases, and eventually leads to zero. The frequency simply increases with  $V_{RF}$ . The highest frequency (25 Hz, beta

rhythm) is reachable at  $V_{RR} = 0.4$ ,  $V_{RF} = 1$ .

Fig. 3(b) diagrams the relation of the synchrony and the connection weights. In the area corresponding to the hyperactive noise region in fig. 3(a),  $k$  is generally zero. In other regions,  $k$  monotonically increases with  $V_{RR}$  and decreases with  $V_{RF}$ . The highest  $k$  always emerges along the edge of hyperactive noise region, where the slow rhythm with large amplitude (fig. 2(c)) was generated.

### 2.2 Synchronization and input intensity

We next examined whether the periodic activity of the column is also affected by the stimulus intensity. The simulations were performed with  $P_{stim}$  changing gradually from 0.01 to 0.05. In fig. 3(c), the oscillation

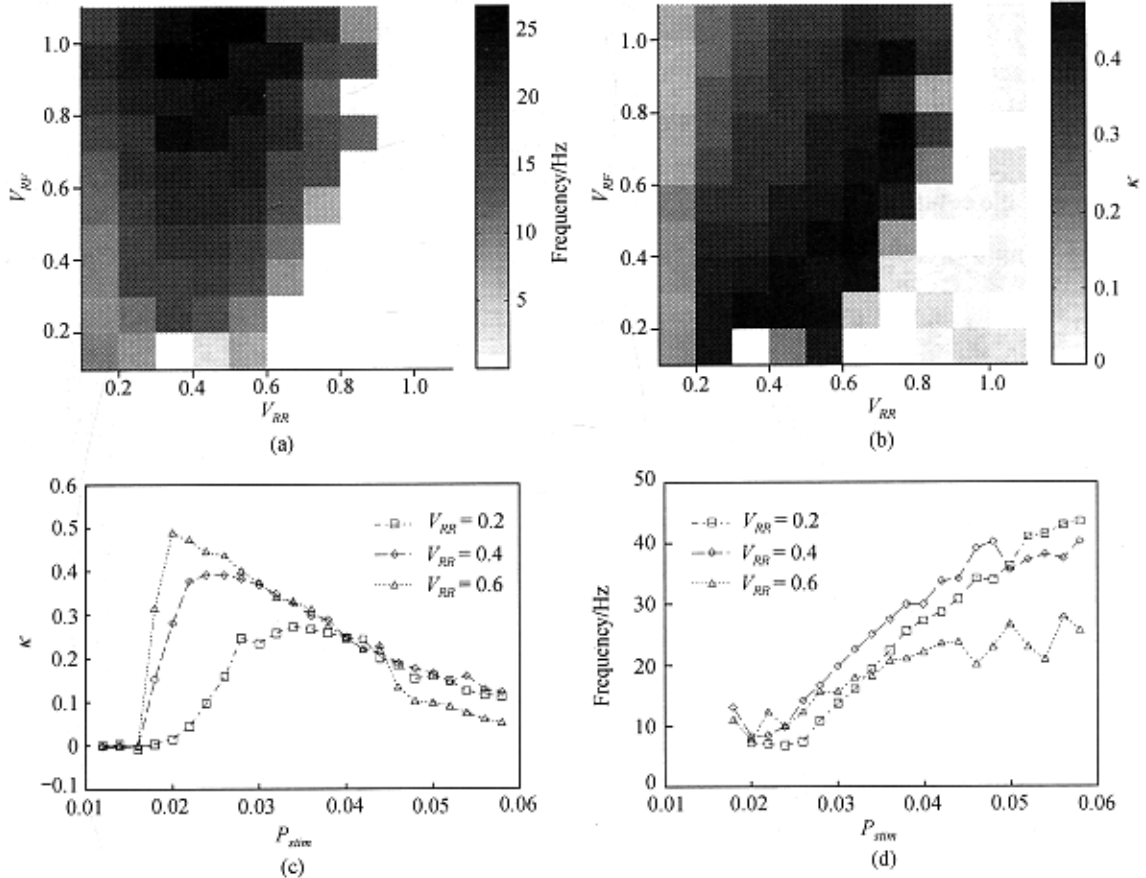


Fig. 3. The dependence of the activity of the column model on the stimulus intensity and the synaptical strength in the excitatory ( $V_{RR}$ ) and inhibitory ( $V_{RF}$ ) feedback loop. (a) Oscillation frequency of the column's activity range from 3 to 20 Hz under different connection weights. (b) The synchrony of the column in the same two-dimensional parameter-space.  $P_{stim} = 0.025$  in (a) and (b). (c) Oscillating frequency versus the input intensity under different levels of  $V_{RR}$ . Increasing input pulse rate leads the column to higher oscillation frequency. (d) The synchrony measure of the column in the same condition as in (c). Minimal input density is required for the network synchronization.  $V_{RF} = 0.4$  in (c) and (d).

frequency of the model is plotted as function of  $P_{stim}$ . The diagram also compares frequency versus  $P_{stim}$  for different levels of  $V_{RR}$ . Only for  $P_{stim}$  larger than a critical point, the oscillation is generated and the frequency generally with  $P_{stim}$  is from 6 Hz to 43 Hz. For greater  $V_{RR}$ , the frequency at smaller  $P_{stim}$  is higher, but the accretion is slower when  $P_{stim}$  increases.

The synchrony measure  $k$  is plotted as a function of  $P_{stim}$  in fig. 3(d).  $k$  is essentially zero for  $P_{stim}$  below a critical value  $\cong 0.016$ . Above the critical value it starts to increase rapidly with  $P_{stim}$  until it reaches a maximum, then decreases inversely until nearly zero at  $P_{stim} = 0.06$ . Thus, the dependence of synchrony on the stimulus intensity is highly non-linear. There is a minimal value of  $P_{stim}$  to generate population synchronization inside a column. This critical  $P_{stim}$  value does not change greatly when the  $V_{RR}$  changes, but greater  $V_{RR}$  significantly accelerate the increase of  $k$  for  $P_{stim}$  larger than the critical value, and the maximum of  $k$  is reached at lower  $P_{stim}$  value for larger  $V_{RR}$ .

### 2.3 Response of the column to periodic stimulation

Sinusoid stimuli were presented to the model

column to explore the behavior of the column responding to periodic input.  $P_{stim}$  is described by eq. (4). The parameters for the column model were kept unchanged at  $V_{RR} = 0.3$ ,  $V_{RF} = 0.8$ ,  $E_{stim} = 0.025$ ,  $A_{stim} = 0.01$ , while the stimulus frequency  $\omega$  varies within 0 and 100 Hz. For  $\omega = 0$  Hz as it has been simulated in section 2.1, the oscillating frequency of the model is defined as inherent frequency of the column. Three kinds of response modes emerged when  $\omega$  changed gradually (fig. 4(a)). The power spectra are arrayed by  $\omega$  in fig. 4(b). to demonstrate the relation between the input frequency and the output frequency. For  $\omega < 10$  Hz, the field potential clearly shows a fast oscillation riding on the peaks of a slow wave. In the power spectrum, besides an obvious peak on the  $y = x$  line, there is another hump around 30 Hz, which is the inherent frequency of the model at the maximal  $P_{stim} = E_{stim} + A_{stim} = 0.04$ . For  $\omega > 10$  Hz and  $< 30$  Hz, in the field potential there is only one rhythm that can be seen. The power spectrum in fig. 4(b) confirms that merely one main peak lies on the  $y = x$  line, besides minor peaks on  $y = kx$  ( $k = 2, 3, 4, 5$ ) lines, which indicates that the column is forced to lock its phase with the

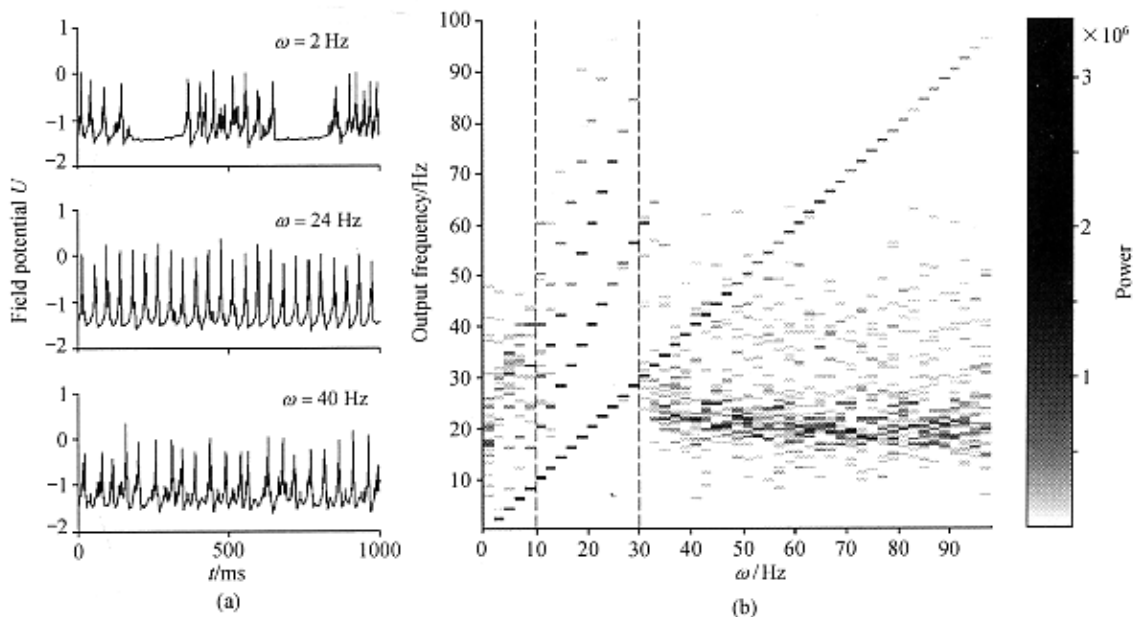


Fig. 4. Response of the column model to periodic stimulation. (a) Several kinds of field potential patterns for different input frequency  $\omega$ . (b) Power spectra of the output rearranged along the abscissa  $\omega$ . The power is diagrammed in pseudo-color.  $V_{RR} = 0.3$ ,  $V_{RF} = 0.8$ ,  $E_{stim} = 0.025$ ,  $A_{stim} = 0.01$ .

input signal. When  $w$  is greater than 30 Hz, another rhythm other than the input one emerges again. On the power spectra diagram it can be seen that a hump appears at around 25 Hz, and as  $w$  increases, the hump gradually decreases and closes in on 20 Hz, the inherent frequency of the column. At the same time, the peak on the diagonal line gradually becomes

dimmer with the increasing  $w$ .

### 3 Simulation results in a multi-column model

A multi-column network is composed by 10 columns, numbered as i, ii, iii, ..., x. The connections between every two columns are all identical. In the following sessions, the simulation was performed for

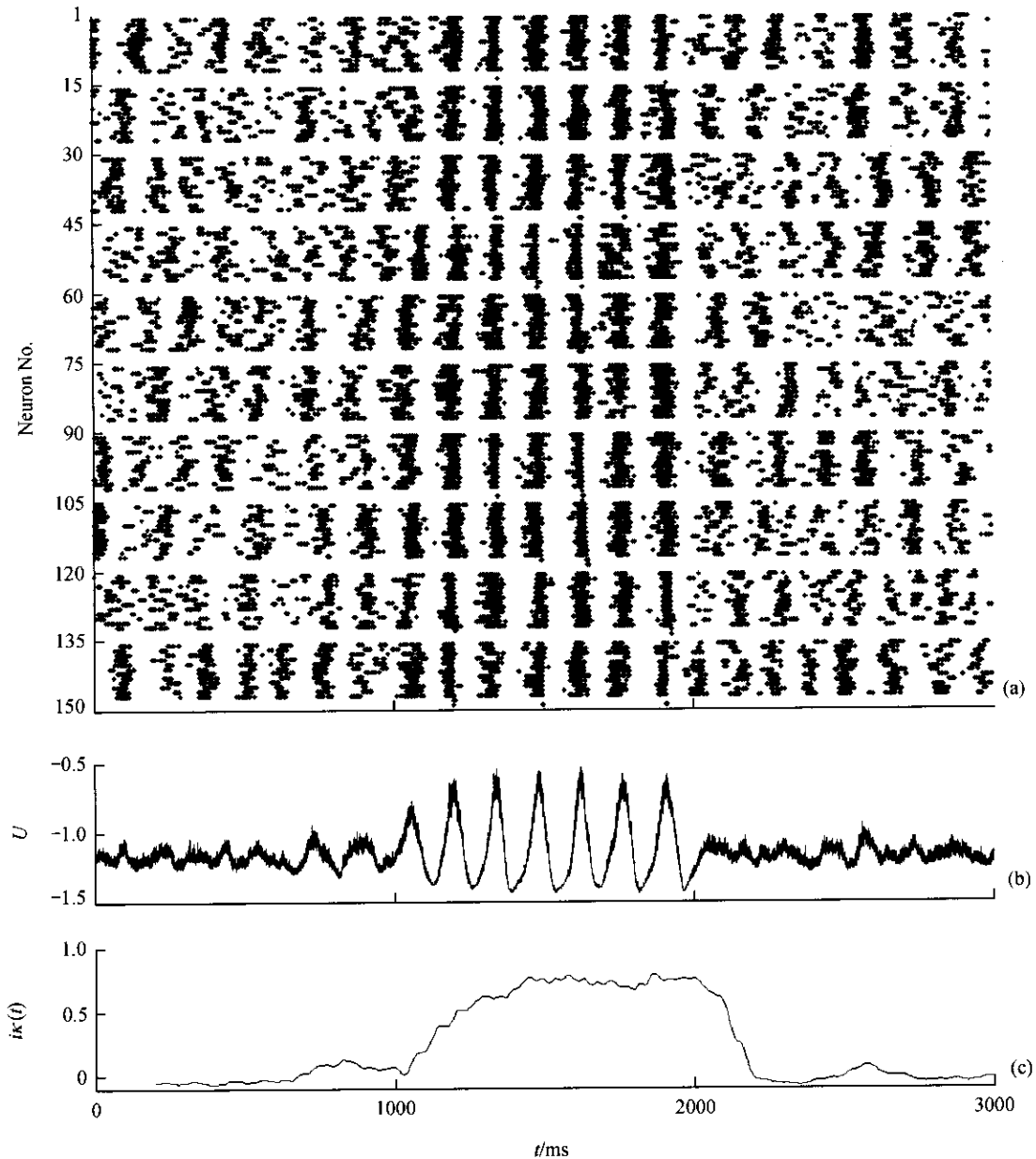


Fig. 5. Interactions among homogeneous columns. (a) Firing pattern of the neurons in the columns. (b) The mean field potential of the ten columns. (c) The instant synchrony measure versus time.  $iV_{RR} = 0.05$  during 1000—2000 ms,  $iV_{RR} = 0$  in the rest time.

3000 ms.  $iV_{RR} = 0.05$  during  $1000 \leq t < 2000$  ms and equals 0 otherwise.

### 3.1 Interaction among homogeneous columns

Homogeneous columns have identical intra-columnar connections, specifically  $V_{RR} = 0.1$ ,  $V_{RF} = 0.3$  in this section. The result in fig. 5(a) indicates that the synchronization is gained among columns even in sparse inter-columnar connections. The mean field potential of the entire ten-column network is illustrated in fig. 5(b), showing an obvious fluctuation during 1000—2000 ms. An instant synchrony measure is introduced to measure the dynamic changing of the synchronization among columns. The zero-lag cross-correlation  $ik_{ij}(t)$  between two columns  $i$  and  $j$  at  $t$  moment is defined as:

$$ik_{ij} = \frac{\int_{t-\Delta}^t (V_i(\mathbf{t}) - \bar{V}_i)(V_j(\mathbf{t}) - \bar{V}_j) dt}{\sqrt{\int_{t-\Delta}^t (V_i(\mathbf{t}) - \bar{V}_i)^2 dt \int_{t-\Delta}^t (V_j(\mathbf{t}) - \bar{V}_j)^2 dt}},$$

where  $V_i(t)$  refers to the field potential of column  $i$  at  $t$  moment,  $\Delta$  is the time bin during which the synchrony is measured,  $\Delta = 200$  ms in this paper. The instant synchrony measure  $ik(t)$  of all the columns is calculated by averaging  $ik_{ij}(t)$  over the number of column pairs in the network. In fig. 5(c),  $ik(t)$  is plotted over time. When the inter-columnar connections take effect,  $ik(t)$  rises from around 0 to approximately 0.7. Both the synchronization and the desynchronization take place immediately.

### 3.2 Interaction among heterogeneous columns

There are a large variety of columns in the cortex. In a cortex area, even neighbor columns are different in properties. We coupled columns with different oscillating properties in a network to investigate the interaction between inhomogeneous rhythms. As shown in fig. 6(a), we use two types of columns which are distinguished by their inner parameter: the five odd-numbered columns (i, iii, v, vii and ix) are alpha-rhythm columns, whose inner coupling strengths were  $V_{RR} = 0.1$ ,  $V_{RF} = 0.3$ , and the frequency of the output is 8 Hz; the rest 5 even-numbered columns are beta-rhythm columns with the parameter  $V_{RR} = 0.5$ ,

$V_{RF} = 0.5$  and an inherent frequency of 18 Hz.

The simulation result is shown in fig. 6. The mean field potential of 5 odd columns (fig. 6(b)) oscillates greatly during 1000—2000 ms, while the mean field potential of even columns (fig. 6(c)) shows no obvious changing.  $ik(t)$  has been calculated among and between the two types of the columns. In fig. 6(d),  $ik_{oo}(t)$ , indicating the instant synchrony among odd columns, rapidly increases to near 0.8 after 1000 ms, and decreases back to around 0 after the inter-columnar connections are removed at 2000 ms. However, the synchrony among even columns  $ik_{ee}(t)$  does not change obviously.  $ik_{oe}(t)$  is the mean  $ik_{ij}(t)$  of all the odd-even-column pairs, indicating the synchrony between the odd columns and the even columns. The variation of  $ik_{oe}(t)$  is almost the same as that of  $ik_{ee}(t)$ . These three measurements show that the synchronization was specifically established among the odd columns.

The above results manifest that, though every two columns are identically and symmetrically connected as they were in the last section, partial synchronization has been found inside the model network.

## 4 Discussion

In the present study a modular neural network model simulates the columnar organization in the cortex. The model column is composed of spiking neurons and the properties of the neurons and connections are based on the physiological data. A single column model generates synchronized rhythm under constant rate of random pulse stimulation. The frequency of the rhythm varies between 3 and 43 Hz by tuning the coupling strength of the excitatory or inhibitory connections and the stimuli intensity. By changing the stimulus frequency we found that the column only responses to a certain range of frequency, in which the column is forced to lose its own inherent frequency and its phase is locked to the input one. The stimuli with the frequency out of the range have little effect on the intrinsic fluctuation of the column. The multi-column network is able to reach global synchronization under sparse inter-columnar projections. Heterogeneous

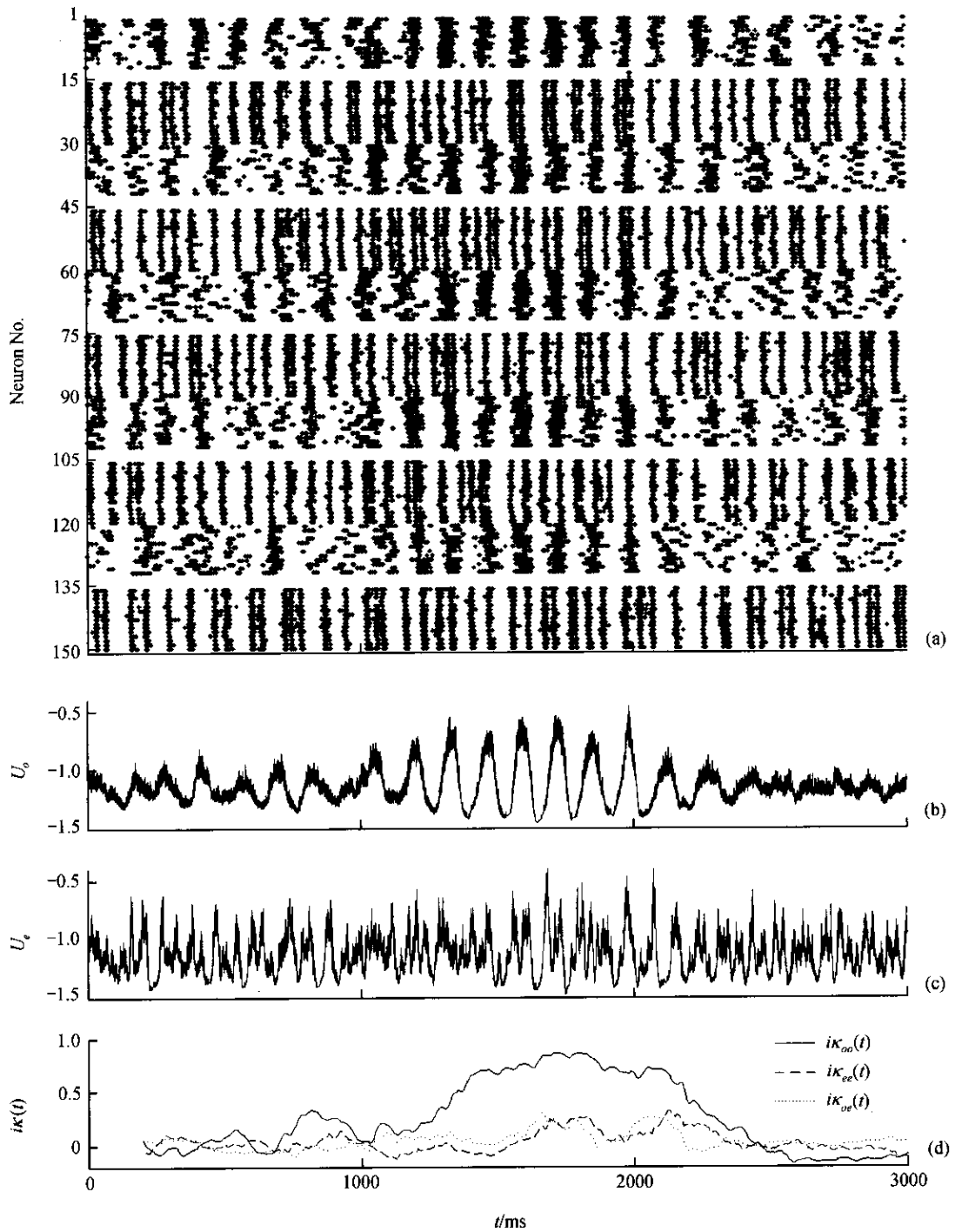


Fig. 6. Interactions among heterogeneous columns. (a) Firing pattern of the neurons in the columns. Set to different coupling strengths, the five odd-numbered columns generate 8 Hz alpha rhythm while the five even-numbered columns generate 18 Hz beta rhythm. (b) The mean field potential of the odd columns. (c) The mean field potential of the even columns. (d)  $iK_{oo}(t)$ , the instant synchrony measure among odd columns;  $iK_{ee}(t)$ , the instant synchrony measure among the even columns;  $iK_{oe}(t)$ , the instant synchrony measure between the odd columns and the even columns.  $iV_{RR} = 0.05$  during 1000—2000 ms,  $iV_{RR} = 0$  in the rest time.

columns, when identically coupled in a network, are partially synchronized and are organized into sub-assemblies based on their intrinsic frequency of the columns.

In most of the previous studies, a column is described through the model developed by Wilson and Cowan. Such a model consists of two nonlinear ordinary differential equations representing two simple units which represent the activities of excitatory and inhibitory neuron populations respectively. This model is able to produce EEG-like rhythms in alpha to beta frequency bands<sup>[6-7]</sup>. The model in this paper is composed of spiking neurons and the properties of the neurons and connections are based on the physiological data. As a result, our column model generates frequencies that are of great diversity, with the range covering most of the EEG bands. The result proves that a cortical column could play a role of an oscillator. In addition, it indicates that the columnar organization provides the possibility of diversity in EEG patterns.

Oscillatory dynamics and the synchronization of neuronal activity are hypothesized to be of functional relevance to information processing in the brain. Von der Malsburg has proposed that these features are linked through temporal correlations of neuronal activities. Each feature is represented by a neuronal group oscillating in a synchronized way, and distinct features of the same object are simultaneously represented by distinct synchronous groups. The column model we proposed is capable of generating sufficient behavior patterns so it is qualified to be a functional unit for a large number of more complex dynamical systems. In the cortex, it is more likely to be columns, instead of individual neurons, that establish contact with each other and carry out the basic function of information processing<sup>[3]</sup>.

Hoppensteadt and Izhikevich<sup>[19]</sup> proposed a hypothesis that the cortex might employ a principle similar to that in FM radio: Each cortical column is an autonomous oscillator. The frequency of oscillation encodes the channel of communication, while the information is transmitted via phase modulations. The results we obtained have shown that the column gen-

erates different rhythms, which is affected by afferent periodic input when there is a nearly resonant relation between the intrinsic and extrinsic frequencies. In an identically coupled multi-column network, a multi-column network can be divided into partial synchronized subgroups by the frequency of the column. Columns in different groups have little effects on each other, although there are synaptic connections between them. These results partially supported the hypothesis. It might provide a new possible mechanism for the information processing in the cortex.

The modern concept of the brain has slowly replaced the point that singles out the neuron as the functional unit of the brain<sup>[20]</sup>. A cortical column is a mesoscopic unit which is smaller than a macroscopic unit as a brain area and is bigger than a microscopic unit as a neuron. To understand such a structure might open a way to connect top-down and bottom-up approaches in brain researches<sup>[21,22]</sup>.

**Acknowledgements** This work was supported by the National Natural Science Foundation of China (Grant Nos. 39893340-06, 30170231 and 62075023), and Brain-Mind Research Center in the Chinese Academy of Sciences.

## References

1. Mountcastle, V. B., Modality and topographic properties of single neurons of cat's somatic sensory cortex, *J. Neurophysiol.*, 1957, 20: 408—434.
2. Buxhoeveden, D. P., Casanova, M. F., The minicolumn hypothesis in neuroscience, *Brain*, 2002, 125: 935—951.
3. Mountcastle, V. B., The columnar organization of the neocortex, *Brain*, 1997, 120: 701—722.
4. Wilson, H. R., Cowan, J. D., Excitatory and inhibitory interactions in localized populations of model neurons, *Biophys.*, 1972, 12: 1—24.
5. Schuster, H. G., Wagner, P., 1: A model for neuronal oscillations in the visual cortex, 2: Phase description of the feature dependent synchronization, *Biol. Cybern.*, 1990, 64: 77—85.
6. Jansen, B. H., Zouridakis, G., Brandt, M. E., A neurophysiologically-based mathematical model of flash visual evoked potentials, *Biol. Cybern.*, 1993, 68: 275—283.
7. Jansen, B. H., Rit, V. G., Electroencephalogram and visual evoked potential generation in a mathematical model of coupled cortical columns, *Biol. Cybern.*, 1995, 73: 357—366.
8. Fukai, T., A model of cortical memory processing based on co-

- lumnar organization, *Biol. Cybern.*, 1994, 70: 427–434.
9. Sompolinsky, H., Golomb, D., Kleinfeld, D., Cooperative dynamics in visual processing, *Phys. Rev. A*, 1991, 43: 6990–7011.
  10. Chawanya, T., Aoyagi, T., Nishikawa, I. et al., A model for feature linking via collective oscillations in the primary visual cortex, *Biol. Cybern.*, 1993, 68: 483–490.
  11. Fransén, E., Lansner, A., A model of cortical associative memory based on a horizontal network of connected columns, *Network: Comput. Neural Syst.*, 1998, 9: 235–264.
  12. Hansel, D., Sompolinsky, H., Chaos and synchrony in a model of a hypercolumn in visual cortex, *J. Comp. Neurosci.*, 1997, 4: 57–79.
  13. Hindmarsh, J. L., Rose, R. M., A model of neuronal bursting using 3 coupled 1st order differential-equations, *Proc. R. Soc. London B*, 1984, 221: 87–102.
  14. Connors, B. W., Gutnick, M. J., Intrinsic firing patterns of diverse neocortical neurons, *Trends Neurosci.*, 1990, 13: 99–104.
  15. Foehring, R. C., Lorenzon, N. M., Herron, P. et al., Correlation of physiologically and morphologically identified neuronal types in human association cortex *in vitro*, *J. Neurophysiol.*, 1991, 66: 1825–1837.
  16. Katz, L. C., Callaway, E. M., Development of local circuits in mammalian visual cortex, *Ann. Rev. Neurosci.*, 1992, 15: 31–56.
  17. White, E. L., *Cortical Circuits: Synaptic Organization of the Cerebral Cortex—Structure, Function, and Theory*, Boston: Birkhäuser, 1989.
  18. Wang, X. J., Buzsáki, G., Gamma oscillation by synaptic inhibition in a hippocampal interneuronal network model, *J. Neurosci.*, 1996, 16: 6402–6413.
  19. Hoppensteadt, F. C., Izhikevich, E. M., Thalamo-cortical interactions modeled by weakly connected oscillators: Could the brain use FM radio principles? *BioSystems*, 1998, 48: 85–94.
  20. Douglas, R. J., Martin, K. A., Opening the grey box, *Trends Neurosci.*, 1991, 14: 286–293.
  21. Freeman, W. J., Mesoscopic neurodynamics: From neuron to brain, *J. Physiol.*, 2000, 94: 303–322.
  22. Freeman, W. J., Rogers, L. J., Holmes, M. D. et al., Spatial spectral analysis of human electrocorticograms including the alpha and gamma bands, *J. Neurosci. Meth.*, 2000, 95: 111–121.

